International Conference on Space Optics—ICSO 2020

Virtual Conference

30 March–2 April 2021

Edited by Bruno Cugny, Zoran Sodnik, and Nikos Karafolas

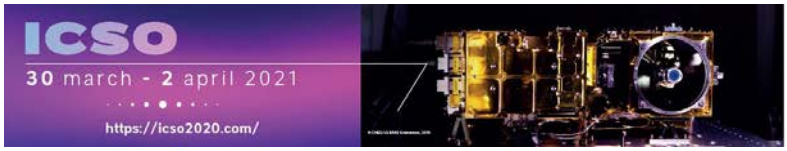

Optimization and additive manufacturing of a three-mirror-anastigmatic telescope

International Conference on Space Optics — ICSO 2020, edited by Bruno Cugny, Zoran Sodnik, Nikos Karafolas, Proc. of SPIE Vol. 11852, 1185206 · © 2021 ESA and CNES
CCC code: 0277-786X/21/$21 · doi: 10.1117/12.2599146

Optimization and Additive Manufacturing of a Three-Mirror-Anastigmatic Telescope

Henrik von Lukowicz[1,2*], Johannes Hartung[1], Enrico Hilpert[1], Christoph Damm[1], Thomas Peschel[1], and Nils Heidler[1]
[1] Fraunhofer Institute for Applied Optics and Precision Engineering IOF, Albert-Einstein-Strasse 7, D-07745 Jena, Germany
[2] Friedrich Schiller University Jena, Institute of Applied Physics Albert-Einstein-Strasse 7, D-07745 Jena, Germany
*Henrik.von.Lukowicz@iof.fraunhofer.de

ABSTRACT

The development of mechanical structures for space telescopes is mainly driven by reducing the mass and in the same step increasing the stiffness [1], thus achieving a high margin of safety against failure during launch and low costs for the satellite mission. These aspects attract more and more attention for the New Space movement, e.g. for constellations of Earth observation and communication systems [2].Considering the state of the art, design of mass-reduced housings is limited by conventional manufacturing processes like CNC-milling [3]. The possibility of additive manufacturing of metallic materials opens the door for an advanced light-weighted design based on topology optimization and thereby, an ideal use of the existing material, which is distributed to optimally sustain loads occurring during launch [3,4]. This article deals with the development, manufacturing, and test of a three-mirror-anastigmatic telescope. In more detail, different concepts for light-weighting will be presented. After the additive manufacturing of the mirrors and housing, the parts can be further processed by the typical process chain (e.g. diamond-turning, plating with electroless nickel), as known from high-performance optics [5-7]. After integration, the mechanical behaviour will be verified with dynamic tests using a shaker and the results (e.g. the eigenfrequencies) will be compared to simulations of a finite-element analysis.

Keywords: telescope, topology optimization, Voronoi foam, additive manufacturing, vibration testing, metal mirror, TMA

1. INTRODUCTION

Currently, the so-called Old Space projects, in which only individual assemblies are manufactured, are the state of the art for optical applications in space. The Fraunhofer IOF develops and manufactures high performance optics for Earth oberservation and interplanetary research like the DESIS telescope and spectrometer, which is oberserving vegetation health or water quality from the ISS since 2018 [8]. Another example for instruments built by the Fraunhofer IOF is the receiver telescope for the Ganymede Laser Altimeter as part of ESA's JUICE mission to explore Jupiter's Icy Moons.

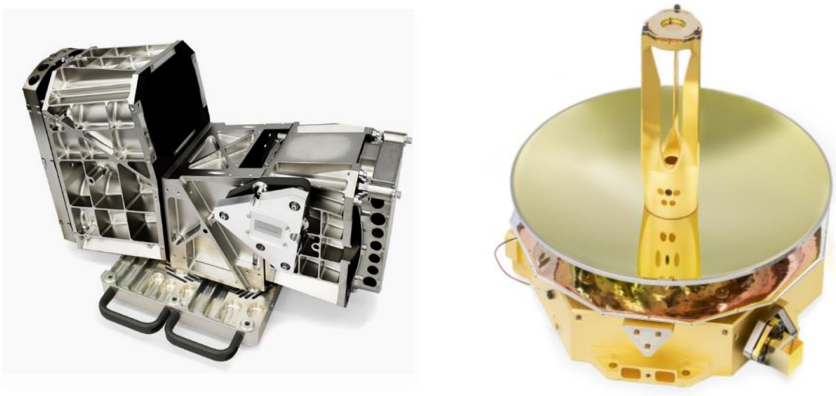

Figure 1: left: DESIS telescope & spectrometer @ ISS; right: GALA RC-telescope @ ESA JUICE

For these systems, a high level of risk mitigation is required. This means, that only well-known processes with a high technological readiness level comes into consideration. Especially for mechanical development regarding light weighting, the design is limited by conventional manufacturing processes like CNC milling.

On the other hand, the area of New Space will launch hundreds of nano satellites [9] (e.g. for laser communication or daily Earth observation [10]) in the next few years. For these satellites, advanced light-weighted and very stiff telescopes (to be more independent from the selection of the launcher) are more important than before and thus, modern technologies like topology optimization and additive manufacturing becoming more and more interesting. These technologies allow for optimal and load-balanced material distribution and can thus increase the specific stiffness of the assembly. Further benefit is be generated by saving manufacturing time and material costs.

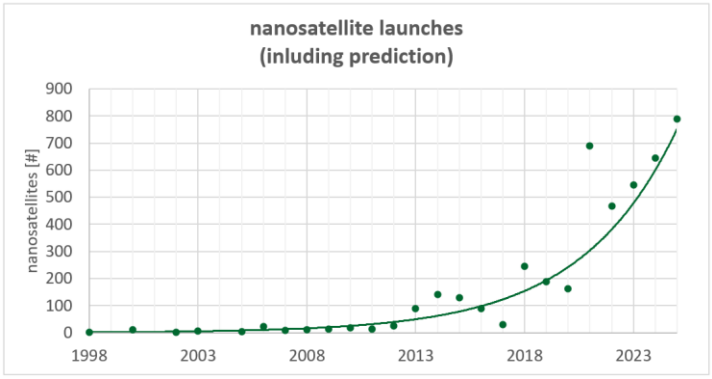

Figure 2: Nanosatellite launches (including prediction) planned for the next few years [9]

2. OPTICAL AND MECHANICAL DESIGN

The telescope used as a benchmark for the optimization follows the principle of a three-mirror-anastigmat (TMA) with a focal length of 175 mm and an F/4 aperture. Such telescopes are typically used in small Earth-observing satellites [11,12]. The TMA relies on three rotationally symmetric aspheric mirrors arranged on a common optical axis. In order to simplify the alignment of the system, two of those mirrors (M1 and M3) will be arranged on a common substrate [13] (see Figure 3).

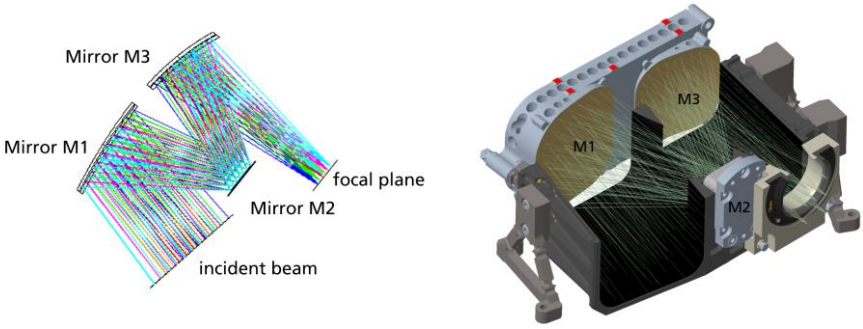

Figure 3: Optical design of the three-mirror-anastigmat (TMA)

The mechanical design of the telescope is based on conventional methods for light-weighting. Thus, a ribbed housing and a cross drilled mirror substrate are used. The mass is about 2 kg and the external dimensions are 210 mm x 130 mm x 110 mm. In addition to the housing, which serves both as a mechanical structure and as a straylight baffle, the mirror substrate M1M3 and the mirror M2 of the telescope consists of bipods as well, which compensate interface errors and thermal gradients.

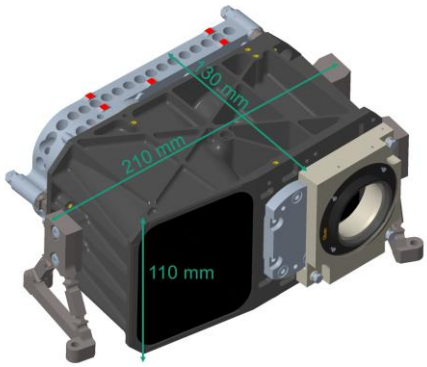

Figure 4: Mechanical design of the TMA with conventional methods for light-weighting

3. OPTIMIZATION

To reduce the mass of the components as far as possible and to make the best possible use of the design freedoms given by the additive manufacturing process, two different optimizations are used. The optimization of the lightweight structure for the M1M3 mirror module is briefly described. The focus is on the topology optimization of the housing.

3.1 Mirrors light-weighted by foam structures

The mirror is filled inside with a stochastic Voronoi foam [14]. The density distribution of the foam is based on static load cases, resulting in a smaller cell size next to the interfaces for mounting at the housing. In addition to the front side, on which the functional areas are located, the backside has a closed surface as well, and thus, a high bending stiffness is generated (see Figure 5).

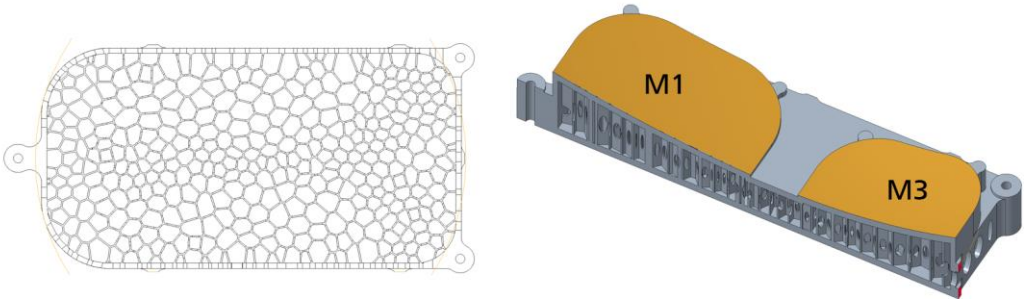

Figure 5: Mirror substrate M1M3 light-weighted by Voronoi foam

The mass could be reduced to 44 % compared to the massive component and is thus slightly below the conventional light-weighted design, which was produced by cross-drilling. In addition, the stiffness can be increased, resulting in a significant increase for the specific stiffness.

Table 1: Mass and eigenfrequencies of the optimized mirror substrate

	massive	cross drilled	Voronoi foam
$m\,[kg]$	0.579	0.256	0.231
$m/m_{Envelope}$	1.00	0.44	0.40
$Freq\,[Hz]$	4666	3290	3650
$Freq/m\ \left[\frac{Hz}{kg}\right]$	8058	12851	15800
$\frac{Freq/m}{Freq_{Envelope}/m_{Envelope}}$	1.00	1.59	1.96

Due to the high eigenfrequencies, which are above the typical incitation frequencies, the substrate is insensitive to random vibration.

3.2 Topology optimization of the housing

For the housing, a topology optimization is used. A defined envelope curve is required for the optimization, in which the material can be manipulated by the optimization algorithm. The envelope has to provide the interfaces to the other components and the straylight baffle, as shown in Figure 6.

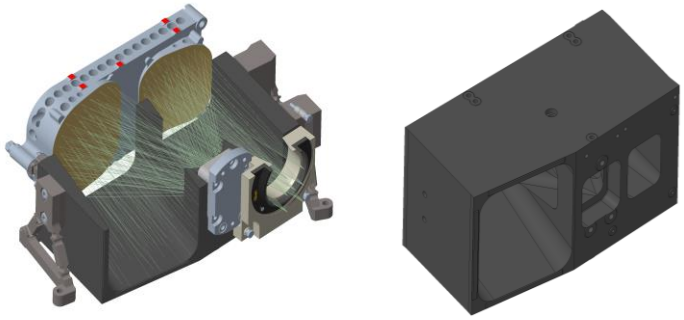

Figure 6: Envelope for the topology optimization of the housing

The most critical load case for this type of mechanical structure is typically random vibration. Since topology optimizations based on random analyses are currently not possible and at the same time the combination of two time-intensive simulations is not reasonable, substitute loads have to be generated. The generation of these substitute loads is similar to a primary notching process, because only the force reaction at the boundary conditions and not the interface forces can be determined in a random analysis.

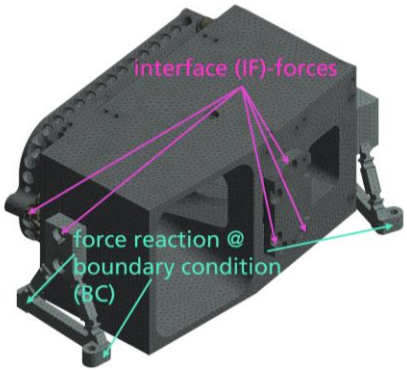

Figure 7: FE-model with envelope and the definition of forces

Because the stresses caused by random vibration depend not only on the excitation, damping, and eigenfrequencies, but also on mass and stiffness, the Young's modulus and density of the envelope are reduced to produce resilient loads. Therefore, the Young's modulus and the density are multiplied by the expected lightweight factor ϕ.

$$E_\phi = E \cdot \phi \qquad \rho_\phi = \rho \cdot \phi \qquad \text{with} \quad \phi = {}^{m}/_{m_{Envelope}} \tag{1}$$

This model is now used to perform random analyses for the x-, y-, and z- directions and the forces reactions at the boundary conditions can be determined. In the next step, the model is accelerated with a quasi-static load (QSL) in x, y, and z and the results are scaled until the same forces occur at the boundary conditions.

$$\sum_{i=1}^{6} \text{Random } f_{bc_i}{}_{x,y,z} \overset{!}{=} \psi_{x,y,z} \cdot \sum_{i=1}^{6} \text{QSL } f_{bc_i}{}_{x,y,z} \tag{2}$$

For the scaled QSL, the interface forces can be simulated and used for topology optimization.

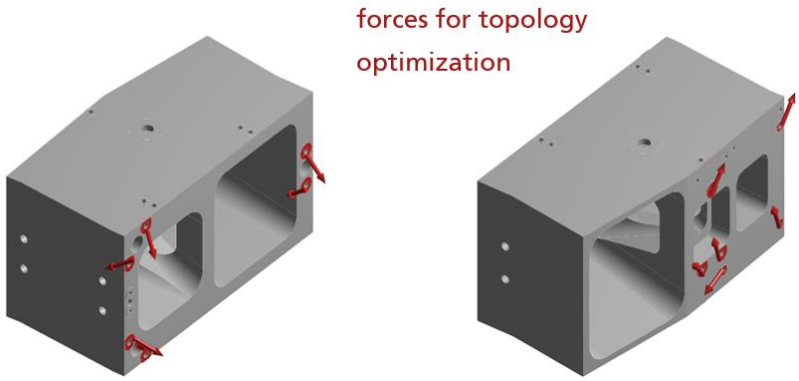

Figure 8: Substitute forces for topology optimization

A fine and uniform mesh is used for the topology optimization. By a linear element order, the number of nodes can be reduced. The increased stiffness of the elements obtained is accepted for the optimization. In the recalculation of the result, a quadratic element order is then used. With an element size of 1.5 mm, the model consists of approx. 1.5 million elements.

The interfaces and the stray light baffle must remain after the optimization and are therefore excluded from the design region.

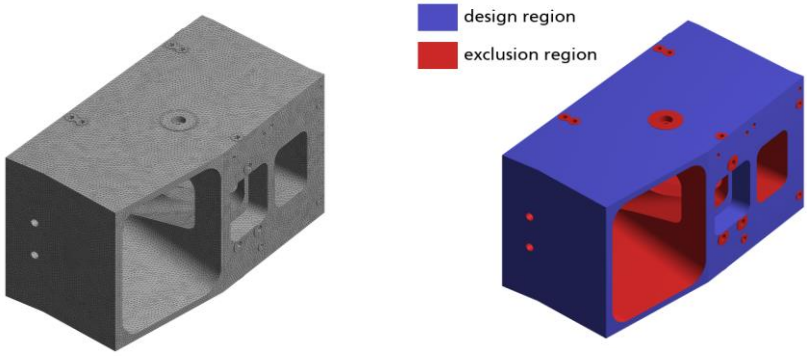

Figure 9 left: uniform mesh; right: design & exclusion region

The following objectives are used for the optimization:

- Lightweight 30 %
- Maximum stress (50 % of yield) under QSL
- Increase 7th mode with free-free conditions
- Increase 1st mode with iso-static mounting
- Minimum structure size: 3 mm

The used quasi-static-loads (QSL) were determined in the previous section. With an increase of the 7th mode under free-free conditions, the result has only six rigid-body modes and thus, a coherent body is obtained. Increasing the 1st mode with iso-static mounting reduces the sensitivity to random vibration. The minimum structure size should be at least twice the element size to avoid hourglass effects.

3.3 Smoothing and regeneration

After optimization, the result must be prepared for additive manufacturing, otherwise the non-continuous removal of elements would result in a very rough surface and there might not be enough material at the interfaces for a subsequent CNC milling process. Three steps are necessary:

1. Repair of small defects, removal of unnecessary elements, and surface smoothing
2. Prepare interfaces (e.g. filling holes) and add additional material for CNC milling
3. Check orientation and generate support structures for additive manufacturing process

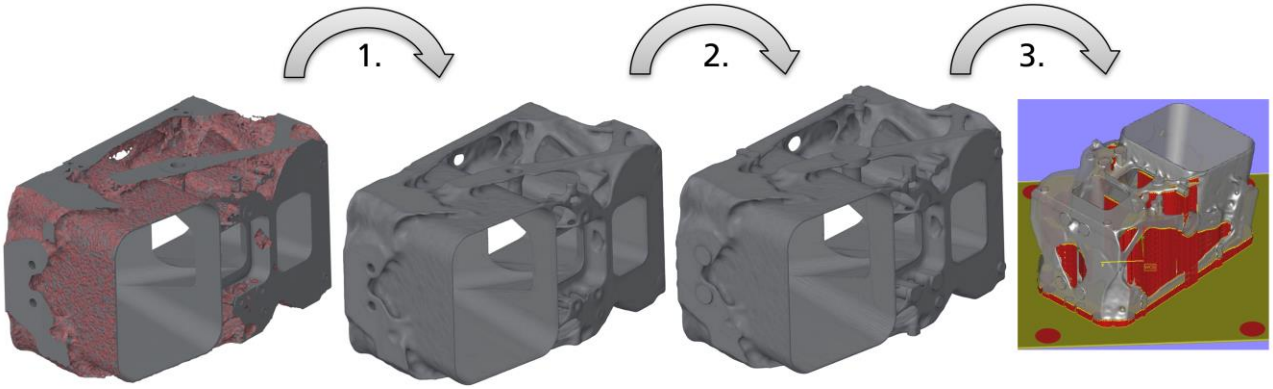

Figure 10: Steps for smoothing and regeneration of the optimized result

3.4 Results of topology optimized housing

After smoothing the model, simulations can be performed with the optimized housing to validate the results. The results of the topology optimization are compared again to the massive envelope model and the conventional ripped housing. Compared to the massive envelope, the mass was reduced to 32 % and thus, the specified lightweight factor of 30 % was well met and is below the mass of the ribbed housing. The difference is more significant for the eigenfrequencies. Thus, the topology-optimized housing is 20 % more stiffly than the ribbed one. In summary, the specific stiffness could also be increased significantly.

Table 2: Mass and eigenfrequencies of the optimized housing

	massive	ribbed	topology optimized
$m\ [kg]$	1.585	0.533	0.502
$m/m_{Envelope}$	1.00	0.34	0.32
$Freq\ [Hz]$	1855	1306	1567
$Freq/m\ \left[\frac{Hz}{kg}\right]$	1170	2450	3121
$\frac{Freq/m}{Freq_{Envelope}/m_{Envelope}}$	1.00	2.09	2.67

The eigenfrequencies were determined under free-free conditions to evaluate the stiffness independent of boundary conditions. The 1st mode shows a global deformation of the housing in each case (see Figure 11).

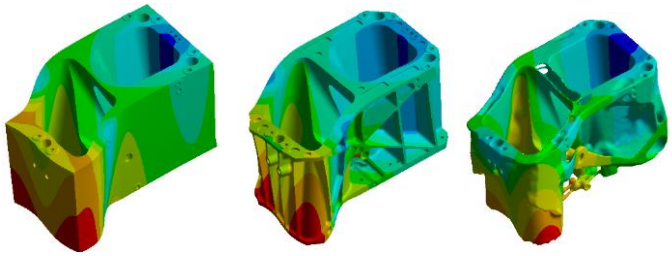

Figure 11: 1st Mode shape of the massive, ripped, and topology optimized housing

4. ADDITIVE MANUFACTURING AND FURTHER PROCESS CHAIN

The mirror and housing are additively manufactured using a selective laser melting (SLM) system as described in [7] and [14]. The parts can be further processed using the established manufacturing chain after removing the support structure. For the housing, this can be only CNC milling and diamond turning of the interfaces. For the mirror substrate, the complete process chain for high performance optics including plating with electroless nickel, shape correction, various polishing processes, and a high-reflective coating is required. The processes work almost independently of whether the component has been produced conventionally with CNC milling or using additive manufacturing. The process chain is shown in Figure 12.

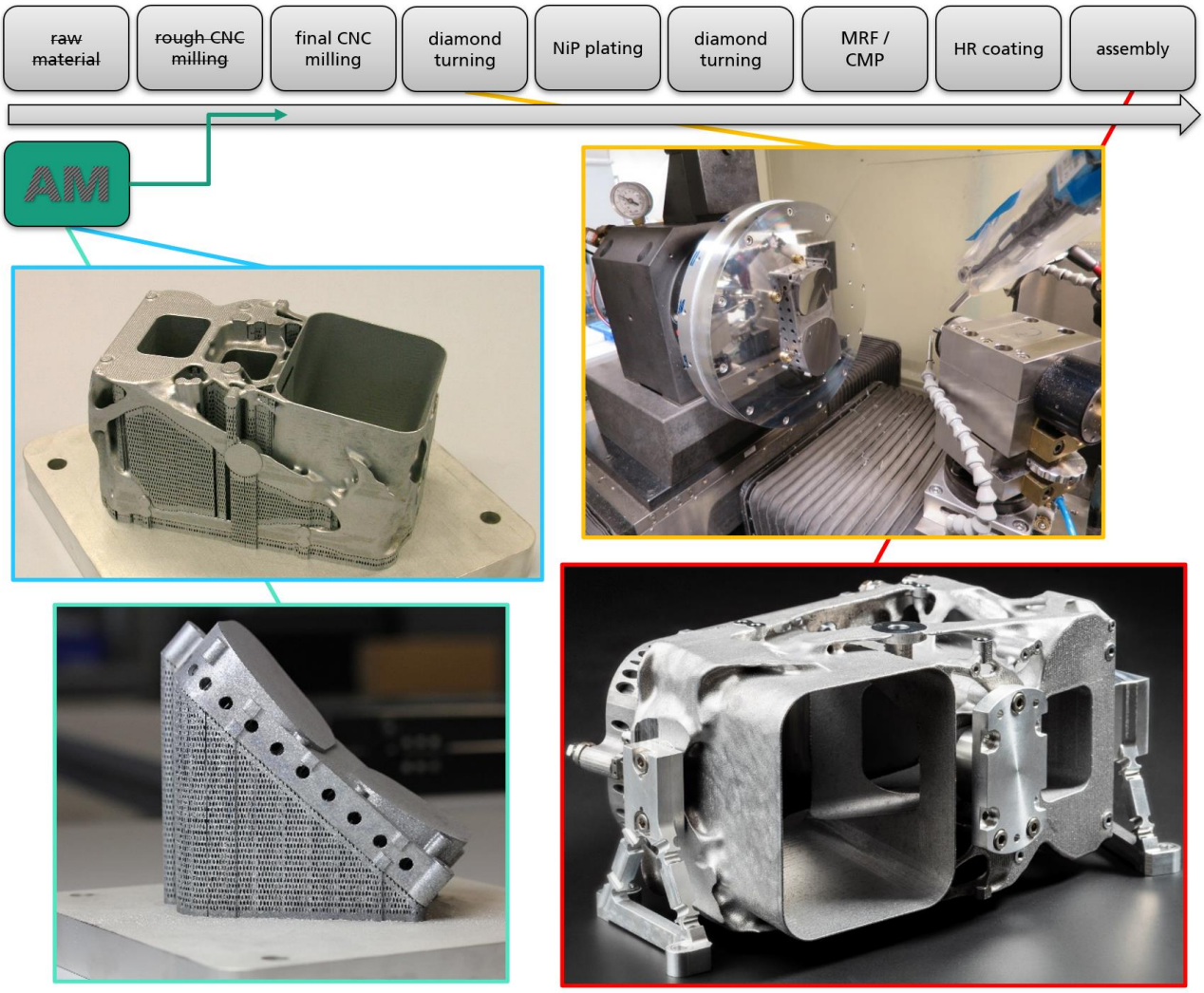

Figure 12: Process chain for additive manufactured mirrors and housing

5. TESTING

In order to validate the FE simulations, especially for such a complex structure, vibration tests are carried out to determine the eigenfrequencies and to verify the load capacity. The test-setup is shown in Figure 13.

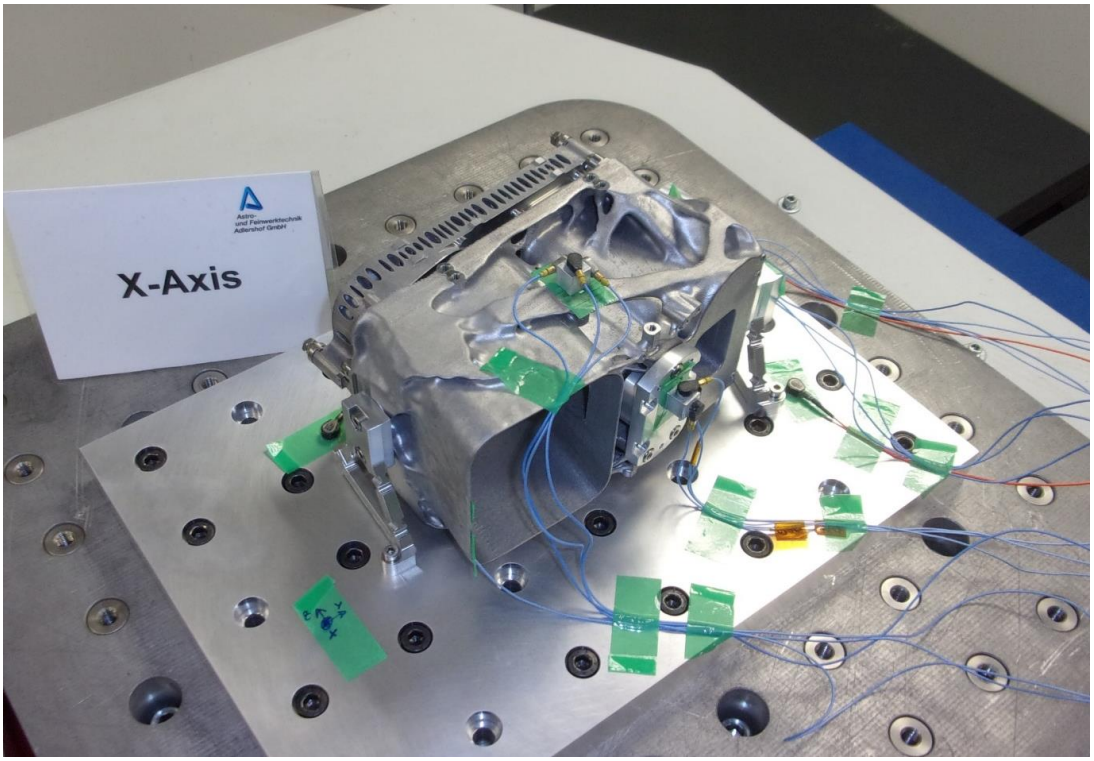

Figure 13: Optimized TMA under vibration testing

5.1 Low-level sine search

For the low-level sine search, the TMA was accelerated in the frequency range 5-2000 Hz with a sine-incitation of 0.5 g. The acceleration sensors show a significant increase of the response acceleration, when reaching the eigenfrequencies due to resonances. The comparison with the simulated harmonic analyses shows that only small deviations below 8 % occur between test and simulation of the eigenfrequency. For most modes, the deviation is much smaller.

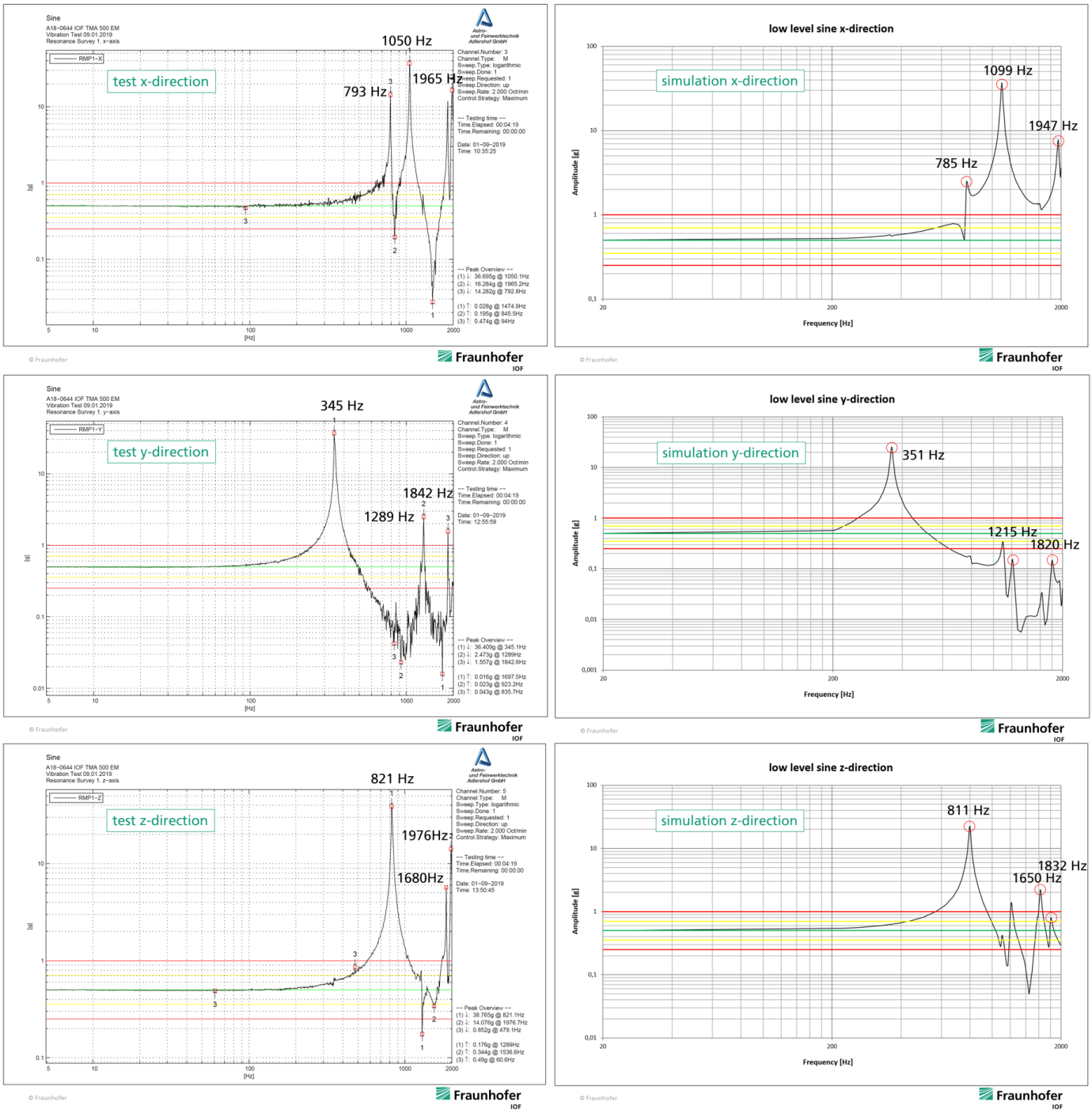

Figure 14: Results of the low-level sine search; left: test; right: simulation

5.2 Random vibration

To verify the loading capacity of the TMA, a random vibration test is performed with a broadband excitation in the x-, y-, and z-directions. A low-level sine test is performed before and after each random load case in order to determine the eigenfrequencies of the TMA. A change in the eigenfrequencies would indicate damage to the assembly.

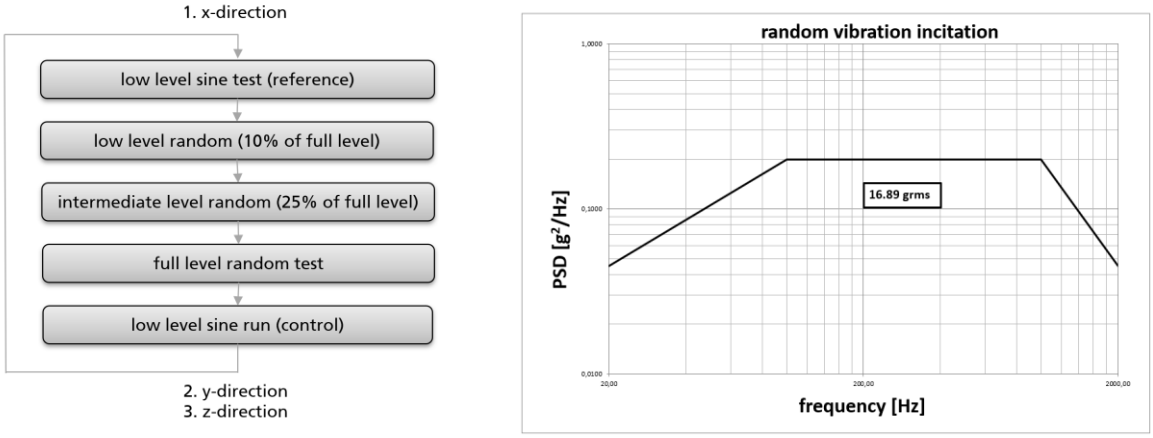

Figure 15 left: test-flow for random vibration testing; right: random spectrum (x-,y-, and z-direction)

The change in the dominant eigenfrequencies (high effective masses in the translatory directions) are less than 1 %. It can therefore be assumed that the TMA is not damaged by the random vibration test.

Table 3: Changes in the dominant eigenfrequencies due to random vibration testing

	reference	control	Delta
Max Eff.-Mass-Mode in X	1050 Hz	1050 Hz	0,00 %
Max Eff.-Mass-Mode in Y	345 Hz	343 Hz	-0,58 %
Max Eff.-Mass-Mode in Z	821 Hz	826 Hz	0,61 %

6. CONCLUSION

The mirror substrate and housing of a three-mirror-anastigmat have been optimized, reducing mass and significantly increasing stiffness compared to a conventional lightweight design. A stochastic Voronoi foam in tow dimensions was used for the mass reduction of the mirror substrate. For the topology optimization of the housing, an approach was presented to generate the required boundary conditions from random analyses. After the additive manufacturing of the components, vibration tests were carried out. The deviation of the eigenfrequencies compared to the FE-simulation was small and within typical deviations for numerical simulations. The random vibration did not cause any damage to the structure.

REFERENCES

[1] H. P. Stahl, "Development of lightweight mirror technology for the next generation space telescope," Proc. SPIE 4451 (2001) 1–4
[2] M. Ehresmann " IRAS: Low-cost Constellation Satellite Design, Electric Propulsion and Concurrent Engineering" IAC-18-B4.6, 2018
[3] A. Ahmad, Ed., Handbook of Optomechanical Engineering. CRC Press, 1997.
[4] L. Berrocal, "Topology optimization and additive manufacturing for aerospace components", Springer Nature, 2018
[5] M. Beier "Fabrication of metal mirror modules for snap-together VIS telescopes", Proc. SPIE 9633, 2015
[6] J. Kinast "Minimizing the bimetallic bending for cryogenic metal optics based on electroless nickel" Proc. SPIE 9151, 2014
[7] E. Hilpert, "Design, additive manufacturing, processing, and characterization of metal mirror made of aluminum silicon alloy for space applications", Optical Engineering Paper 190152SS, 2019
[8] DLR DESIS website, (https://www.dlr.de/eoc/desktopdefault.aspx/tabid-13614)
[9] Nanosat website, (www.nanosats.eu)
[10] ConstellR website, (https://constellr.space/)
[11] S. Kirschstein, A. Koch, J. Schöneich, F. Döngi, "Metal Mirror TMA –Telescopes of the JSS product line: Design and Analysis", Proc. of SPIE Vol. 5962, 59621M, 2005
[12] M. Francois, S. Santandrea, K. Mellab, D. Vrancken, J. Versluys, "The PROBA-V mission: the space segment", Int. Journal of Remote Sensing 35, 2548, 2014
[13] S. Risse, S. Scheiding, A. Gebhardt, C. Damm, W. Holota, R. Eberhardt, A. Tünnermann, "Development and fabrication of a hyperspectral, mirror based IR-telescope with ultra-precise manufacturing and mounting techniques for a snap-together system assembly", Proc. SPIE 8176, 81761N, 2011
[14] Heidler, N.; Hilpert, E.; Hartung, J.; et al., "Additive manufacturing of metal mirrors for TMA telescope," Proc. SPIE 10692, 2018